INTERNATIONAL SOCIETY FOR SOIL MECHANICS AND GEOTECHNICAL ENGINEERING



This paper was downloaded from the Online Library of the International Society for Soil Mechanics and Geotechnical Engineering (ISSMGE). The library is available here:

https://www.issmge.org/publications/online-library

This is an open-access database that archives thousands of papers published under the Auspices of the ISSMGE and maintained by the Innovation and Development Committee of ISSMGE.

The paper was published in the proceedings of the 20th International Conference on Soil Mechanics and Geotechnical Engineering and was edited by Mizanur Rahman and Mark Jaksa. The conference was held from May 1st to May 5th 2022 in Sydney, Australia.

Experimental study on the microbial cementation of desert aeolian sand cementation under different calcium sources

Etude expérimentale sur la cimentation microbienne de la cimentation des sables éoliens du désert sous différentes sources de calcium

Hongxian Gou

Associate Professor, Department of Civil Engineering, Tsinghua University, Beijing, China

Xichen Xu

Ph.D. Student, Department of Civil Engineering, Tsinghua University, Beijing, China

Meng Li

Associate Professor, Key Laboratory of Cosmetic, China National Light Industry, College of chemistry and materials engineering, Beijing Technology and Business University, Beijing, China

ABSTRACT: This study aims at improving the loose aeolian sand via microbially induced carbonate precipitation (MICP), and investigating the precipitated crystals polymorph and microstructures of bio-cemented sands under different calcium sources. In this study, *Sporosarcina pasteurii* is selected as the ureolytic bacterial strain to produce urease, since previous studies indicate that *Sporosarcina pasteurii* can significantly enhance soil mechanical behaviors. Then calcium chloride and calcium acetate are used as cementation sources providing calcium ions to precipitate calcium carbonate crystals. The results of unconfined compressive test show that to cement loose aeolian sand particles, the efficiency of calcium acetate is as favorable as that of calcium chloride. However, the calcium carbonate crystal polymorphs and morphologies precipitated by calcium chloride and calcium acetate are different. The X-ray diffraction (XRD) and scanning electron microscope (SEM) results indicate rhombohedral calcite crystals are precipitated by calcium chloride to act as the solid bridges among the sand particles, while apart from the calcite, acicular aragonite crystals are also formed under the promotion of calcium acetate. Additionally, along with the increase of the cementation solution amount, the size of calcite crystals become larger, and the aragonite crystals appear to be clusters.

RÉSUMÉ: Cette étude vise à améliorer le sable éolien meuble via la précipitation de carbonate induite par des microbes (MICP), et à étudier la polymorphie et les microstructures des cristaux précipités des sables bio-cimentés sous différentes sources de calcium. Dans cette étude, Sporosarcina pasteurii est sélectionnée comme souche bactérienne uréolytique pour produire de l'uréase, car des études antérieures indiquent que Sporosarcina pasteurii peut améliorer considérablement les comportements mécaniques du sol. Ensuite, le chlorure de calcium et l'acétate de calcium sont utilisés comme sources de cémentation fournissant des ions calcium pour précipiter les cristaux de carbonate de calcium. Les résultats du test de compression non confiné montrent que pour cimenter les particules de sable éolien en vrac, l'efficacité de l'acétate de calcium est aussi favorable que celle du chlorure de calcium. Cependant, les polymorphes et morphologies des cristaux de carbonate de calcium précipités par le chlorure de calcium et l'acétate de calcium sont différents. Les résultats de la diffraction des rayons X (XRD) et du microscope électronique à balayage (MEB) indiquent que les cristaux de calcite rhomboédrique sont précipités par le chlorure de calcium pour agir comme des ponts solides entre les particules de sable, tandis qu'en dehors de la calcite, des cristaux aciculaires d'aragonite sont également formés sous le promotion de l'acétate de calcium. De plus, avec l'augmentation de la quantité de solution de cémentation, la taille des cristaux de calcite devient plus grande et les cristaux d'aragonite semblent être des amas.

KEYWORDS: Aeolian sand, calcium chloride, calcium acetate, unconfined compressive strength, crystal polymorph

1 INTRODUCTION

Building roads and controlling surface erosion in desert are extremely difficult, since the loose structure of aeolian sand and terrible weather in the desert environment will hinder the construction. Thus, solidification of loose aeolian sand is necessary prior to construction. Compared with traditional approaches, microbially induced carbonate precipitation (MICP) acting as a state-of-the-art ground improvement technology, can be applied in an environmentally friendly way, since the biobased materials are with good degradation, and favorable efficiency achievement (Wang et al., 2017; Zhan et al., 2020). TO date, the MICP technique has applied to the wind erosion control, slope stabilization, ground improvement, and so on (Tian et al., 2018; Jiang et al., 2019; Feng and Montoya, 2017; Montoya et al., 2014; Gowthaman et al., 2019).

As revealed by previous investigation (Stocks-Fischer et al., 1999; DeJong et al., 2014), the MICP process relies on the

ureolytic bacteria to hydrolyze urea. Then, the released carbonates attract free calcium ions thus precipitating calcium carbonate crystals which act as the solid bridges to cement loose sand particle together. This bio-chemical process can be presented as following equations:

$$CO(NH_2)_2 + 2H_2O \rightarrow 2NH_4^+ + CO_3^{2-}$$
 (1)
 $Ca^{2+} + CO_3^{2-} \rightarrow CaCO_3 \downarrow$

Researchers devoted to optimizing the MICP process in order to save resources, time, and cost, meanwhile achieve a favorable efficiency. From a bacterial perspective, *Sporosarcina pasteurii* is the most popular bacterial strain due to the high urease activity, and Achal et al, (2009) developed a mutant of *Sporosarcina pasteurii* to further enhance the urease activity of *Sporosarcina pasteurii* thereby precipitating more calcium carbonate. While, it has been reported that a higher calcium ions concentration may inhibit the capacity of ureolytic bacteria to hydrolyze urea (Al-Thawadi, 2008). To solidifying aeolian sand, Duo et al. (2018)

examined five different concentrations (0.5, 1.0, 1.5, 2.0 and 2.5 M) of cementation solution, then finding the 2M calcium chloride-urea can achieve highest strength. Additionally, Zhang et al. (2015) investigated the effects of different calcium sources on MICP, pointing that calcium acetate is a great alternative calcium source to cement sand particles. However, the efficiency of calcium acetate on the aeolian sand has not been examined. Consequently, this study uses calcium chloride and calcium acetate to provide calcium ions, then examines their effects on the strength improvement. Moreover, different batches of MICP injection are conducted, then the microstructure changes of biocemented aeolian sands are observed via X-ray diffraction (XRD) and scanning electron microscope (SEM) tests.

2 MATERIALS AND METHOD

2.1 Materials

The sand particles cemented in this study were sampled from the Hobq Desert, Ordos, Inner Mongolia Autonomous Region, China. The particle size distribution and its composition are shown in Figure 1 and Figure 2 respectively. It can be seen that above 95% of aeolian sand particles own sizes from 0.1mm to 0.4mm; quartz (SiO₂) is the main composition of aeolian sand, and a small amount of other minerals such as albite, microcline, and cordierite.

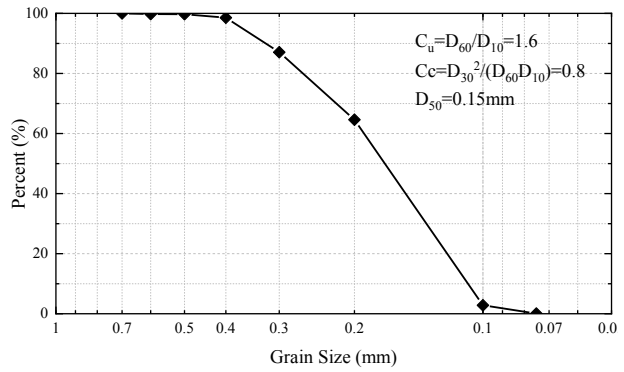


Figure 1 Particle size distribution of aeolian sand

This bacterial strain used in the current study is *Sporosarcina pasteurii*, which was purchased from the American Type Culture Collection (ATCC) with a strain number of ATCC-11859. The culture medium to grow bacteria contains 20 g /L yeast extract, 10 g /L (NH4)2SO4 and 10 µmol NiCl2, and the pH is adjusted to 8.5 to 9 through NaOH. After stirring via a magnetic stirrer, the prepared culture medium was sterilized in an autoclave at 120°C for 20 min, then was taken out from the autoclave and put into clean bench to inoculate. Finally, the inoculated culture medium was put into a shaking cultivation at 30 °C, with an agitation speed of 180 rpm, for 16 hours to obtain the bacterial suspension.

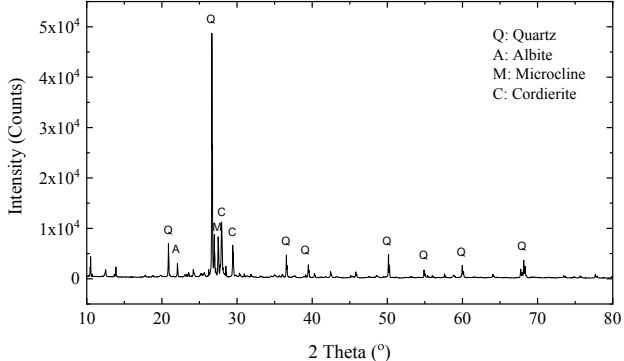


Figure 2 Aeolian sand composition

2.2 Method

2.2.1 Microbial treatment

The sample preparation and microbially injection procedure are similar to those described in Xu et al. (2020). Detailed experimental scheme is shown in Table 1. For each group (A1 group), there are three replicates (A1-1, A1-2, and A1-3).

Table 1 Experimental scheme							
ID	Cementation solution Batch Total cementation solution volume						
A1 A2 A3	0.5M Urea/ 0.5M Ca lcium acetate	1 2 3	500 1000 1500				
C1 C2 C3	0.5M Urea/ 0.5M Ca lcium chloride	1 2 3	500 1000 1500				

2.2.2 Unconfined compressive test

After finishing the MICP injection, the bio-cemented samples were taken from the columns, then dried in the oven at 70°C for 48 hours. Moreover, prior to the unconfined compressive test, the upper and lower surfaces of bio-cemented samples were smoothed. The unconfined compressive test was conducted through a Material Test System 810 (MTS810) in Building Materials Laboratory of Tsinghua University. The axial load was applied at a constant rate of 0.3 mm/min. The broken bio-cemented samples were collected for the further investigations including calcium carbonate content, XRD, and SEM tests.

2.2.3 Calcium carbonate content measurement

The acid-rinsed method was used to measure the calcium carbonate content of a bio-cemented sample. Approximately 5g broken bio-cemented part were taken from the middle of a bio-cemented sample, then placed on a filter paper. After drying at 70°C for 24 hours, the weight of bio-cemented sample and filter paper was measured (m₁). Next, the HCl solution was added to dissolve the bio-cemented samples until no bubbles was generated. Subsequently, deionized water was used to flush the remaining samples. Finally, both sand particles and filter papers were put in the oven, and dried at 70°C for 24 hours, then the dry weight of them was noted as m₂. Thus, the calcium carbonate content of each sample was calculated following:

$$CaCO_3 = \frac{m_1 - m_2}{m_2} \times 100\%$$

2.2.4 *Diffraction of X-rays*

Diffraction of X-rays (XRD) tests were investigated in the Material Laboratory Center of Tsinghua University (model D/max-2500/PC). The selected bio-cemented samples were crushed into powders and screened by a No. 400 sieve. During the XRD test, the scan range was between 20° and 70°, and the scan speed was 5° /min.

2.2.5 Scanning electron microscope

Scanning electron microscopes (SEM) tests were conducted in the Material Laboratory Center of Tsinghua University, and the model is *Merlin Compact*. The selected bio-cemented samples were broken, then the ones with relatively smooth surfaces were prepared to be the SEM samples. Prior to the SEM tests, all samples were stuck to a copper plate then sputtered with gold coatings.

3 RESULTS AND DISCUSSION

The results of unconfined compressive strength (UCS) and calcium carbonate content (CCC) are shown in Table 2. The low UCS of the C1-1 sample maybe caused by its inherent uneven

distribution of calcium carbonate. Moreover, the blockage happens in the third injection of A3 group, which leads to the low UCS and CCC results.

Table 2 Experiment results							
ID	UCS (MPa)	CCC (%)	ID	UCS(MPa)	CCC (%)		
A1-1	4.16	22.97	C1-1	0.42	24.65		
A1-2	3.99	25.63	C1-2	5.78	34.04		
A1-3	5.98	24.35	C1-3	5.99	39.70		
A2-1	8.92	35.37	C2-1	18.97	46.33		
A2-2	12.14	48.58	C2-2	12.88	52.49		
A2-3	21.39	46.89	C2-3	15.14	45.67		
A3-1	17.33	33.73	C3-1	14.60	50.63		
A3-2	10.33	33.60	C3-2	17.43	52.38		

C3-3

21.98

53.66

3.1 Unconfined compressive strength

4.97

A3-3

The average unconfined compressive strength (UCS) of each group are presented in Figure 3. Note that the samples in A-3 group were clogged around the injection areas, thus the cementation solution cannot be fully injected.

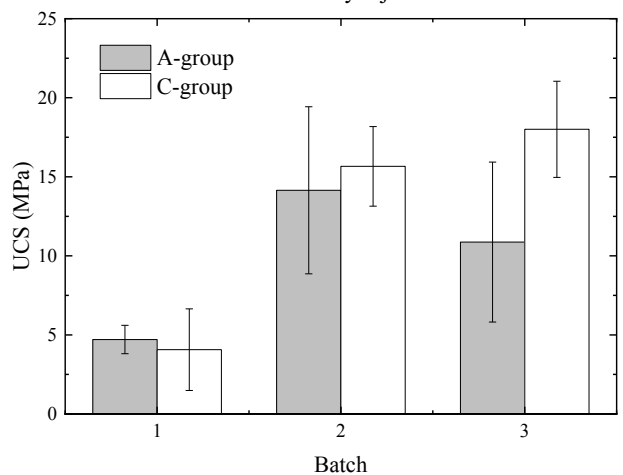


Figure 3 The average UCS of each group

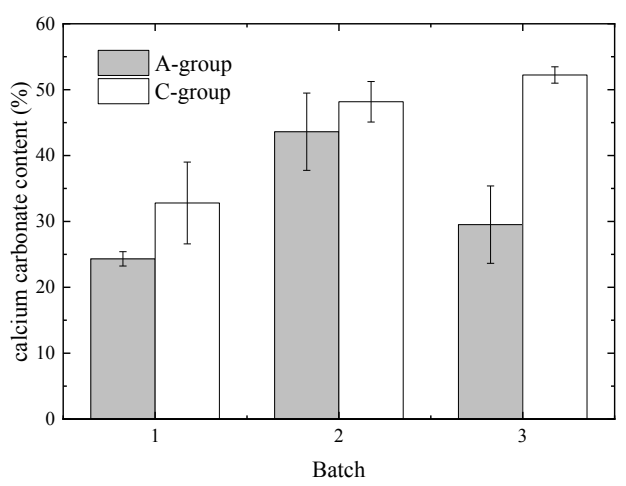


Figure 4 The average calcium carbonate content of each group

For the bio-cemented samples treated by one batch and two batch, the average UCS of A-group is similar to that of C-group. For A-1 group, the average UCS of samples cemented by calcium acetate is slightly higher than that treated by calcium choride. While, the results of A-2 group are inverse. Therefore, in term of the strength improvement, the calcium acetate is also a favorable

calcium source to provide calcium ions. Additionally, it should be noted that the usage of calcium acetate can avoid the threat of chloride ions.

3.2 Calcium carbonate content

The average calcium carbonate contents of each group are presented in Figure 4. Since during the third injection batch, clog happened to the A3 group and the cementation solution was not fully injected, thus the calcium carbonate content of A-3 group is greatly lower. For A-1 and A-2 groups, the average calcium carbonate contents are lower than these of C-1 and C-2 groups respectively. It can be explained by that the calcium chloride is a strong electrolyte, which can provide more free calcium ions to combine with carbonate groups, thereby precipitating more calcium carbonate.

Additionally, the calcium carbonate contents of bio-cemented samples related to UCS are shown in Figure 5, where the bio-cemented samples were collected for SEM and XRD tests are labeled. As revealed by previous investigation, the UCS has a positive relationship with the amount of calcium carbonate content. However, for the samples with the same amount of calcium carbonate contents, the UCS of bio-cemented sand sample belong to A-group is possibly larger than that of sample in C-group.

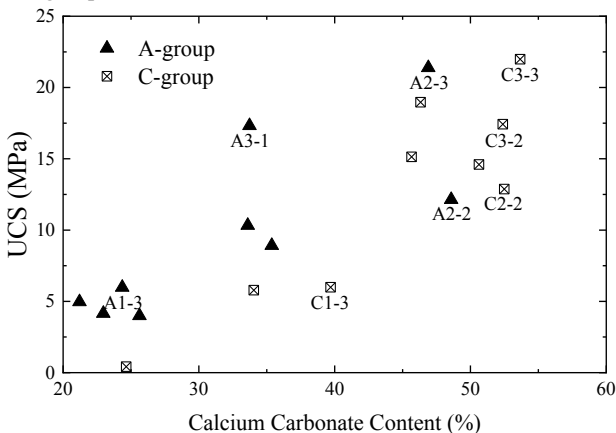


Figure 5 Calcium carbonate contents of bio-cemented samples

3.3 Bio-cemented microstructure

3.3.1 Crystal polymorph

The XRD patterns of six representative samples are presented in Figure 6. Due to the difficulties of separating aeolian sand particles and calcium carbonate, the compositions of aeolian sand, thus a small amount of SiO₂ are also shown in the XRD patterns.

As can be seen, the calcium carbonate crystals precipitated by calcium acetate (A-group) are calcite and aragonite, where the aragonite contents increase along with the amount of cementation solution. While, as for the C-group where the calcium chloride acted as the calcium source, calcite crystals are the single calcium carbonate polymorph.

3.3.2 Crystal morphology and microstructures of biocemented samples

The SEM images for A group and C group are shown in Figure 7 and Figure 8, respectively.

For the bio-cemented samples treated by calcium acetate, Figure 7(a) (b) and (c) indicate that the thicknesses of calcium carbonate coatings increase along with the injection of cementation solution amount. It can be seen from Figure 7(a) that the bio-cemented sample still keep voids, while the sand particles shown in Figure 7(c) are covered by the dense calcium carbonate

coatings thus the voids or pores are difficult to identify.

As can be seen, the calcium carbonate crystals precipitated by calcium acetate (A-group) are rhombohedral calcite and acicular aragonite; while the calcium carbonate crystals of C-group are rhombohedral calcite crystals. Additionally, along with the increase of cementation solution, the crystal morphology is gradually changed. To be specific, for A1-3 (Figure 7(d)) which treated by 500ml cementation solution, the calcite crystal sizes range from $1\mu m$ to $2\mu m$, and the aragonite crystals appear acicular. However, when the cementation solution reaches to 1000ml, it can be seen that the crystals attaching the surfaces of sand particles are still within $1\mu m$ to $2\mu m$, but with the increase of distance to the sand particle surfaces, the crystals the calcite

crystals grow to $10\mu m$, even $15\mu m$. Then, for A3-group (Figure 7(f)), the aragonite morphology is slightly changed. Although aragonite crystals are still in the shape of acicular, they aggregate and form clusters. Another finding is that as shown in Figure 7(d) and (e), aragonite crystals look like grow from calcite surfaces, but the more detailed crystallization process needs to be further examined. Compared with the calcite crystals precipitated by calcium acetate (Figure 7) under the same amount of cementation solution, the calcite crystals of C-groups is larger. For example, the calcite crystals of C1-group are closed to $15\mu m$, even larger than $20\mu m$. And the change of crystal size along with the amount of cementation solution is not obvious.

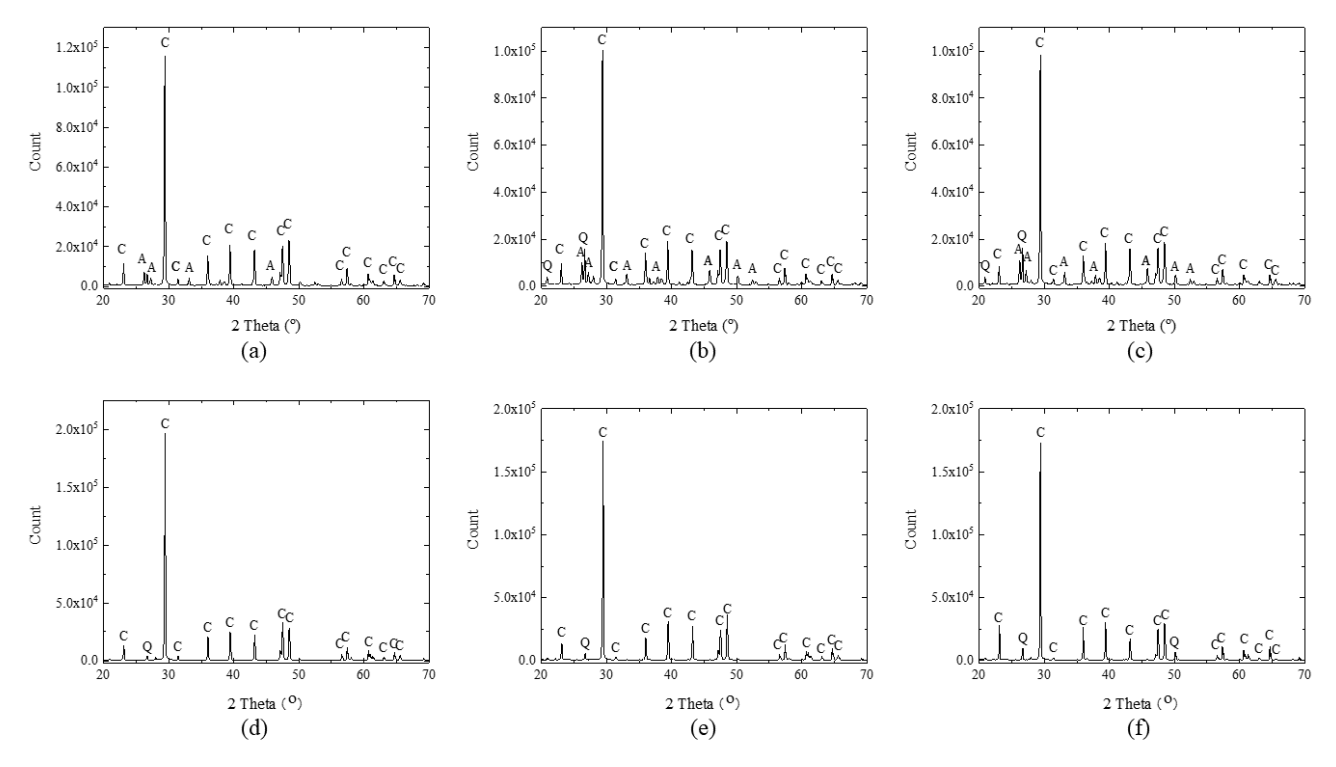


Figure 6 XRD patterns where C is calcite, A is aragonite, and Q is quartz: (a) is sampled from A1-3, (b) is sampled from A2-3, (c) is sampled from A3-1, (d) is sampled from C1-2, (e) is sampled from C2-2, and (f) is sampled from C3-3.

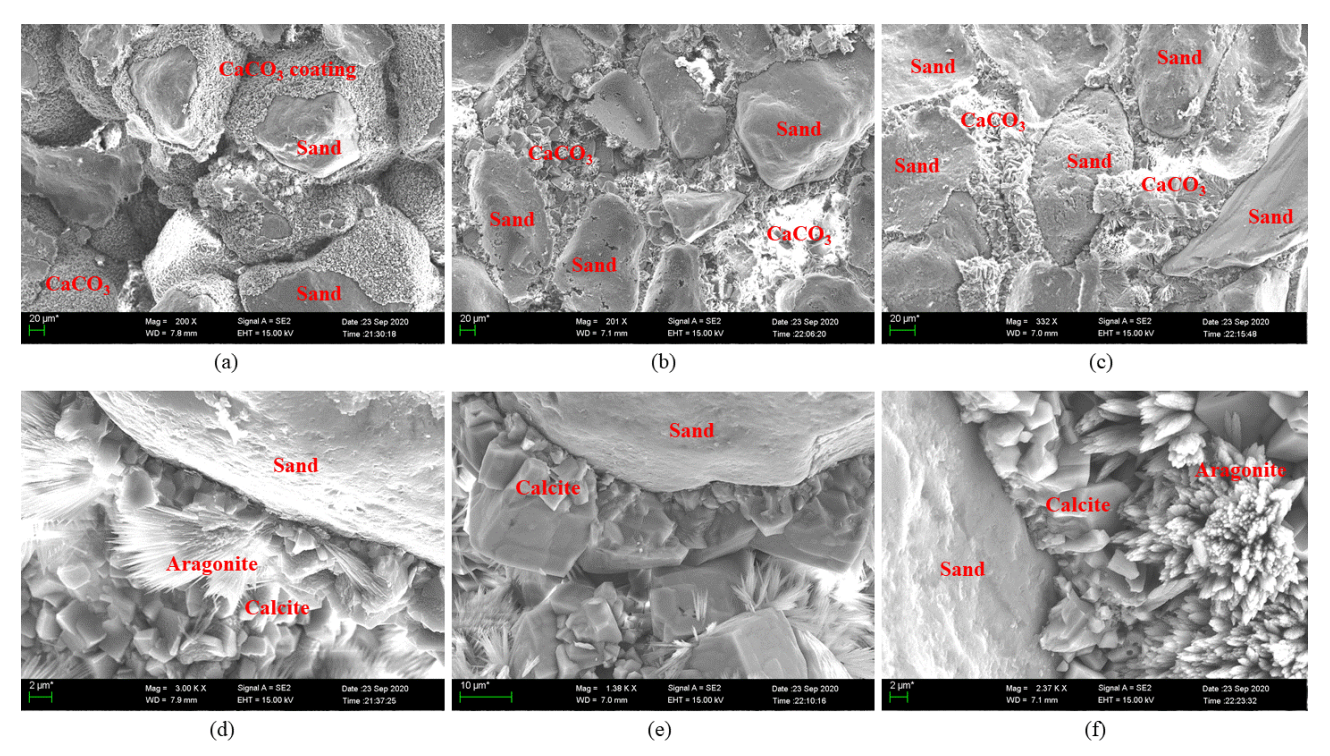


Figure 7 SEM images for A-group bio-cemented samples, where (a) and (d) are sampled from A1-3, (b) and (e) are sampled from A2-3, and (c) and (f) are sampled from A3-1.

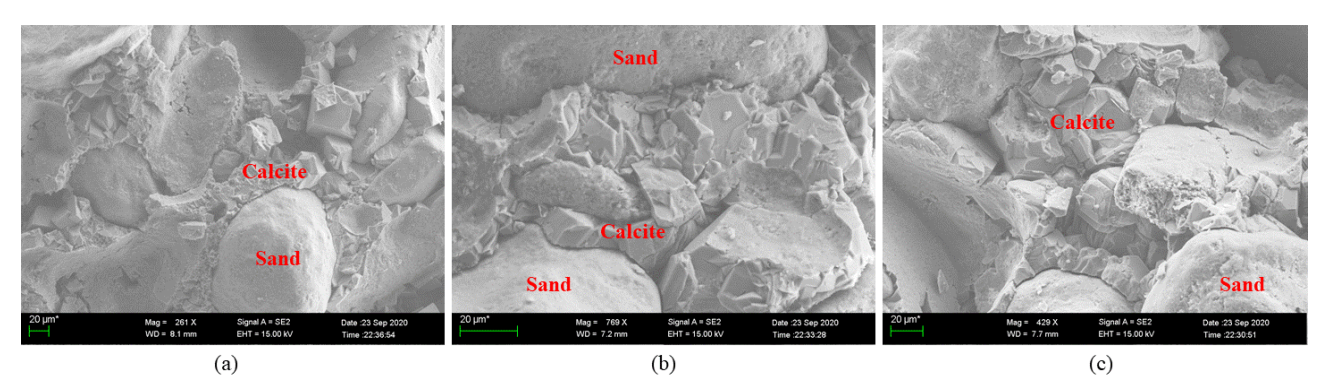


Figure 8 SEM images for C-group bio-cemented samples, where (a) is sampled from C1-2, (b) is sampled from C2-2, and (c) is sampled from C3-3.

4 CONCLUSIONS

This study primary investigates the efficiency of bio-cementation under different calcium sources (calcium chloride and calcium acetate) from mechanical behaviors and microstructures of biocemented sand samples.

The results indicate the average unconfined compressive strength of bio-cemented samples treated by calcium chloride and calcium acetate is similar, but the calcium carbonate precipitated by calcium chloride is more than that by calcium acetate. This is probably attributed to the different calcium carbonate crystal polymorphs. As revealed by the XRD and SEM results, acicular aragonite and rhombohedral calcite crystals are precipitated when calcium acetate acts as the calcium source. Meanwhile the aragonite percentage within a bio-cemented sample increases with the cementation solution amount. Additionally, the size of calcite crystal also increases with the injection of cementation solution. However, for the calcium carbonate crystals precipitated by calcium chloride, rhombohedral calcite crystal is the single phase, and the size of the calcite is larger than that precipitated by calcium acetate.

Moreover, based on the SEM images, it seems the aragonite

crystal begin to grow from the calcite surface, but more detailed investigation is needed to prove the crystallization process.

5 ACKNOWLEDGEMENTS

Funding for this research includes financial funding from the Project (No. 044007003) and National Natural Science Foundation of China (No.51978381).

6 REFERENCES

Achal, V., Mukherjee, A., Basu, P. C., & Reddy, M. S. (2009). Strain improvement of Sporosarcina pasteurii for enhanced urease and calcite production. *Journal of industrial microbiology & biotechnology*, 36(7), 981-988.

Al-Thawadi, S. (2008). High strength in-situ biocementation of soil by calcite precipitating locally isolated ureolytic bacteria (Doctoral dissertation, Murdoch University).

DeJong, J. T., Soga, K., Kavazanjian, E., Burns, S., Van Paassen, L. A., Al Qabany, A., ... & Chen, C. Y. (2014). Biogeochemical processes and geotechnical applications: progress, opportunities and challenges. In Bio-and Chemo-Mechanical Processes in Geotechnical Engineering: Géotechnique Symposium in Print

- 2013 (pp. 143-157). Ice Publishing.
- Duo, L., Kan-liang, T., Hui-li, Z., Yu-yao, W., Kang-yi, N., & Shi-can, Z. (2018). Experimental investigation of solidifying desert aeolian sand using microbially induced calcite precipitation. Construction and Building Materials, 172, 251-262.
- Feng, K., & Montoya, B. M. (2017). Quantifying level of microbialinduced cementation for cyclically loaded sand. *Journal of Geotechnical and Geoenvironmental Engineering*, 143(6), 06017005.
- Gowthaman, S., Iki, T., Nakashima, K., Ebina, K., & Kawasaki, S. (2019). Feasibility study for slope soil stabilization by microbial induced carbonate precipitation (MICP) using indigenous bacteria isolated from cold subarctic region. SN Applied Sciences, 1(11), 1480.
- Jiang, N. J., Tang, C. S., Yin, L. Y., Xie, Y. H., & Shi, B. (2019). Applicability of microbial calcification method for sandy-slope surface erosion control. *Journal of Materials in Civil Engineering*, 31(11), 04019250.
- Montoya, B. M., DeJong, J. T., & Boulanger, R. W. (2014). Dynamic response of liquefiable sand improved by microbial-induced calcite precipitation. In Bio-and Chemo-Mechanical Processes in Geotechnical Engineering: Géotechnique Symposium in Print 2013 (pp. 125-135). ICE Publishing.
- Stocks-Fischer, S., Galinat, J. K., & Bang, S. S. (1999). Microbiological precipitation of CaCO3. Soil Biology and Biochemistry, 31(11), 1563-1571.
- Tian, K., Wu, Y., Zhang, H., Li, D., Nie, K., & Zhang, S. (2018). Increasing wind erosion resistance of aeolian sandy soil by microbially induced calcium carbonate precipitation. *Land Degradation & Development*, 29(12), 4271-4281.
- Wang, Z., Zhang, N., Cai, G., Jin, Y., Ding, N., & Shen, D. (2017).
 Review of ground improvement using microbial induced carbonate precipitation (MICP). Marine Georesources & Geotechnology, 35(8), 1135-1146.
- Xu, X., Guo, H., Cheng, X., & Li, M. (2020). The promotion of magnesium ions on aragonite precipitation in MICP process. Construction and Building Materials, 263, 120057.
- Zhan, Q., Yu, X., Pan, Z., & Qian, C. Microbial-induced synthesis of calcite based on carbon dioxide capture and its cementing mechanism. *Journal of Cleaner Production*, 278, 123398.
- Zhang, Y., Guo, H. X., & Cheng, X. H. (2015). Role of calcium sources in the strength and microstructure of microbial mortar. *Construction and Building Materials*, 77, 160-167.